JOURNAL OF SOLID STATE CHEMISTRY **122,** 371–375 (1996)
ARTICLE NO. 0129

Structure Analysis of the Twin-Free Orthorhombic $YBa_2Cu_3O_{7-x}$ Single Crystals

Wen-Jye Jang, Hatsumi Mori, Masaya Watahiki, Setsuko Tajima, Naoki Koshizuka, and Shoji Tanaka

Superconductivity Research Laboratory, ISTEC 1-10-13 Shinonome Koto-ku, Tokyo 135, Japan

Received September 8, 1995; accepted December 20, 1995

The electron density maps of the twin-free orthorhombic $YBa_2Cu_3O_{7-x}$ single crystal were calculated from the refinement of X-ray structure analysis. The $YBa_2Cu_3O_{7-x}$ single crystal was grown by the top-seeded crystal pulling method. Uniaxial pressure was applied in the oxygen annealing process to manufacture a twin-free orthorhombic single crystal. The crystal structure of $YBa_2Cu_3O_{7-x}$ with a superconducting transition temperature of 91 K was determined by a four-circle X-ray diffractometer. Crystal data are as follows: M_r, 666.4; orthorhombic; *Pmmm*; $a = 3.8278(7)$, $b = 3.8952(7)$, $c = 11.711(2)$ Å; $V = 174.61(5)$ Å^3; $Z = 1$; $D_x = 6.317$ Mg^{-3}; λ(Mo$K\alpha$) = 0.71069 Å; μ(Mo$K\alpha$) = 282.77 cm^{-1}. The final values of the weighted reliability factor (R_w) and unweighted factor (R) were 0.031 and 0.026, which enables us to analyze Fourier difference maps. In the Fourier difference maps it was found that two electrons in the $3d_{z^2}$ orbital of Cu2 are not dumbbell-like but are localized as a lone pair and that the inclined electron density around the O2 atom gives polarization along the *c* axis but not around the O3 atom.

INTRODUCTION

Since the discovery of the high-T_c superconductivity of $YBa_2Cu_3O_{7-x}$ (1), many experiments of crystal growth for YBCO have been reported, but all the crystals were thin plates with small size along the *c* axis (2–4). Recently, large single crystals along the *c* axis were grown by flux methods (5, 6) and by a top-seeded pulling method (7). The X-ray diffraction measurement for polycrystalline samples indicates that the crystal symmetry of YBCO changes from tetragonal to orthorhombic at 600°C with reducing temperature (8). While samples are cooled from the tetragonal phase to the orthorhombic phase, a twin structure is introduced. Most of the structural analyses were performed for the tetragonal phase (9–14) and the orthorhombic phase of twinned crystals (15, 16) or the oxygen deficient crystal with $x = 0.45$ (17), and the weakly twinned orthorhombic phase which contained a certain amount of twinning (18). Twin-free crystal are required to determine the difference of physical properties between the *a* and the *b* directions. For detwinning, the most popular technique is to apply a uniaxial pressure along the *a* direction. For this purpose a large single crystal, particularly long along the *c* axis, is required. We have grown a large YBCO single crystal by a pulling technique (7) and detwinned it by applying uniaxial pressure in the oxygen annealing process. Using this crystal, we have studied the electron density of the $YBa_2Cu_3O_{7-x}$ single crystal by an X-ray diffraction analysis. In this paper, the first report of crystal structure analysis of a twin-free orthorhombic YBCO single crystal is presented and it's electron density maps are discussed.

EXPERIMENTAL

The as-grown crystal was cut into a small piece with a size of $1.5 \times 1 \times 2$ mm^3 and polished before annealing at 500°C in O_2 atmosphere for 130 hr. Uniaxial pressure of about 3×10^6 N/m^2 was applied along the *a* direction in the oxygen annealing process to obtain a twin-free orthorhombic single crystal for X-ray analysis. The temperature dependence of the susceptibility was measured by a dc magnetometer (SQUID) in the applied field H = 10 Oe parallel to the *c* axis. The specimen was cooled to 10 K under a zero field and then susceptibility was measured, applying a field of 10 Oe (zero-field cooling measurement). The composition of metals was determined by inductively coupled plasma atomic emission spectrometry (ICP).

A single crystal shaped into $0.04 \times 0.04 \times 0.01$ mm^3 was taken out for the crystal structure analysis. The intensity data were collected by the 2θ-ω scan method, using a Rigaku Rotaflex AFC-5 four-circle diffractometer (50 kV, 180 mA) with Mo$K\alpha$ radiation ($\lambda = 0.71069$ Å) monochromatized by graphite. A scan speed was 4°/min. The range of *hkl* values measured was $0 \le h \le 9$, $0 \le k \le 9$, and $-28 \le l \le 28$. Among the 3072 reflections measured, 1147 reflections with $F \ge 5\,\sigma(F)$ were used for refinement after absorption correction by ψ-scan. A correction for secondary extinction was applied with a coefficient of 2.98053×10^{-6}. The structure was solved by using Fourier techniques included in the DIRDIF program (19). Neutral

0022-4596/96 $18.00

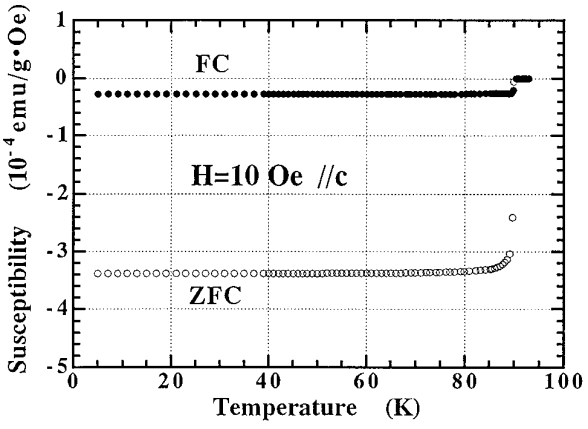

FIG. 1. Temperature dependence of the susceptibility of the annealed YBCO crystal for the applied field H = 10 Oe parallel to the *c* axis. ZFC and FC represent the data for the zero-field cooling and the field cooling, respectively.

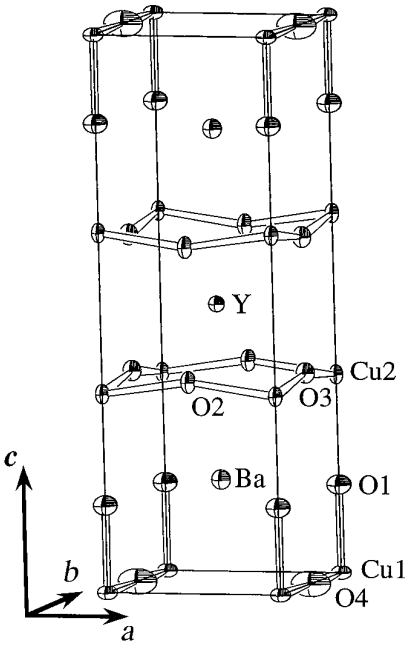

FIG. 2. Twin-free YBCO crystal structure at 90% probability level for the data set Table 1.

atom scattering factors were taken from Cromer and Waber (20). Anomalous dispersion effects were included in F_c (21); the values for $\Delta f'$ and $\Delta f''$ were from Creagh and McAuley (22).

RESULTS AND DISCUSSION

The twin-free orthorhombic single crystal exhibits a superconducting transition at 91 K (Fig. 1). The result of the ICP measurement gave the composition ratio as $Y_1Ba_{2.06}Cu_{3.07}O_{7-x}$ and the small amount of impurities as 0.04 wt% of Mg and 0.02 wt% of Sr. However, the structure refinement for the site multiplicity in the X-ray analysis showed that the chemical formula can be written as $Y_1Ba_{2.02}Cu_{2.98}O_{6.92}$ by fixing the occupancies of Y, O1, O2, and O3 (Table 1). The thermal parameters for all atoms indicate that $\beta_{22} < \beta_{11}$ except for Cu2, O1, and O2 which are different from $\beta_{11} = \beta_{22}$ in the tetragonal phase. Figure 2 shows the structure diagram using the data from Table 1. The long axes in thermal ellipsoids of O2, O3, and Cu2 are along the *c* axis. On the other hand, the short axes in the thermal ellipsoids of O1, Cu1, and O4 are along the *c* axis. It is consistent with it's cleavage nature on the (001) plane. The thermal ellipsoid of Ba and Y atoms is near spherical.

The structure of YBCO is known to be described as two-oxygen-deficient ABO_3 perovskite. One defect is located at (0, 0, 0.5) and the other is O5 (0.5, 0, 0). In the case of the twin crystal, however, the structure analysis indicates that

TABLE 1
Atomic Coordinates, Anisotropic and Equivalent Isotropic Temperature Coefficients, and Site Occupation Factors

Atom	Y	Ba	Cu1	Cu2	O1	O2	O3	O4
x	0.5	0.5	0	0	0	0.5	0	0
y	0.5	0.5	0	0	0	0	0.5	0.5
z	0.5	0.18470(2)	0	0.35530(4)	0.1578(2)	0.3791(2)	0.3782(2)	0
β_{11}[a]	0.0059(2)	0.00870(7)	0.0092(3)	0.0041(1)	0.013(1)	0.0046(9)	0.0078(9)	0.039(4)
β_{22}	0.0052(2)	0.00668(7)	0.0070(2)	0.0042(1)	0.013(1)	0.0086(9)	0.0044(8)	0.008(2)
β_{33}	0.00061(2)	0.000914(8)	0.00045(2)	0.00095(2)	0.0009(1)	0.0013(1)	0.0011(1)	0.0017(2)
B_{eq}[b]	0.472(2)	0.328(5)	0.42(2)	0.334(5)	0.69(3)	0.49(3)	0.45(3)	1.22(7)
occ.	1	2.016(2)	0.986(3)	1.989(4)	2	2	2	0.92(1)

Formula: $Y_1Ba_{2.016(2)}Cu_{2.975(7)}O_{6.92(1)}$ a = 3.8278(7) Å, b = 3.8952(7) Å, c = 11.711(2) Å, V = 174.61(5) Å^3, (this work)

[a] $T_a = \exp\{-(h^2\beta_{11} + k^2\beta_{22} + l^2\beta_{33})\}$; T_a, anisotropic temperature factor.
[b] $T_i = \exp(-B_{eq} \sin^2 B/\lambda^2)$; T_i, isotropic temperature factor.

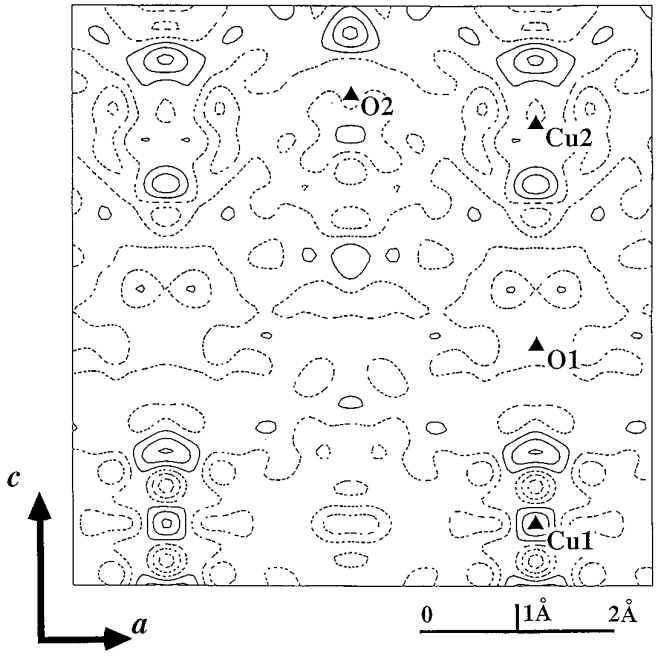

FIG. 3. Fourier difference map of twin-free YBCO crystal shown in the (010) plane at $y = 0$. Contour intervals 1 eÅ^{-3}. Contours in positive regions are solid and negative regions are dashed; zero contour is omitted.

the O5 site is not vacant because of the mixing of *ab* axes. However, in our twin-free crystal, no oxygen is observed at the O5 site, which is proved by the Fourier difference map shown in Fig. 3. The crystal structure analysis proved that our single crystal is perfectly twin-free.

The interatomic distance of the twin-free YBCO crystal is shown in Table 2. The bond distance of Y–O2 is longer than that of Y–O3, the bond distance of Ba–O2 is also slightly longer than that of Ba–O3, and the distance of Cu2–O3 is larger than that of Cu2–O2. The Cu2 atom is coordinated to one O1, two O2's and two O3's, where the oxygen atoms form a pyramid. Note that the distance of Cu2–O1 is 2.312(3) Å, which is much longer than Cu2–O2 (1.9341(4)) and Cu2–O3 (1.9660(5)). This means that the Cu2–O1 bond is much weaker than other Cu–O bonds. Concerning the Ba atom, the distances of Ba–O3 as well as Ba–O2 are longer than those of Ba–O1 and Ba–O4. Therefore, the Ba–O2 and the Ba–O3 bonds are also weak. This also supports it's cleavage nature parallel to (001). The distance of Cu1–O1 is the shortest among Cu–O bonds, so the Cu1–O1 bond is stronger than the others.

TABLE 2
Interatomic Distances (Å) of Twin-Free YBCO Crystal

Ba–O1	2.7486(4) × 4	Cu1–O1	1.849(3) × 4
–O2	2.996(2) × 2	–O4	1.9476(3) × 1.8
–O3	2.996(2) × 2		
–O4	2.8882(2) × 2	Cu2–O1	2.312(3) × 1(?)
		–O2	1.9341(4) × 2
Y–O2	2.408(2) × 4	–O3	1.9660(5) × 2
–O3	2.387(2) × 4		

The final cycle of full-matrix least-squares refinement was converged with unweighted and weighted R values,

$$R = \Sigma \,||F_c| - |F_o||/\Sigma\,|F_o| = 0.026$$

$$R_w = \sqrt{(\Sigma\omega(|F_o| - |F_c|)^2/\Sigma\omega F_o^2)} = 0.031,$$

where F_o is the observed crystal-structure factor and F_c is the calculated crystal-structure factor. The Fourier difference maps were drawn using the $|F_o| - |F_c|$ values obtained in the final step of the refinement. Figures 3 and 4 show the Fourier difference map and the Fourier map in the (010) plane at $y = 0$ for the twin-free orthorhombic single crystal. Figures 5 and 6 show the Fourier difference maps in the (100) and (110) planes. The contour interval for mapping is 1 eÅ^{-3}. The highest positive and lowest negative peaks in our Fourier difference maps appear around the Ba atom with the electron density differences $\Delta\rho$ of 5.0 and -4.0 eÅ^{-3}. Other positive and negative peaks appear around the Y, Cu1, and Cu2 atoms with $\Delta\rho$ of about 3.0 and -3.0 eÅ^{-3}. As mentioned above, in the (010) plane (Fig. 3), there is no residual peak at the O5 site between the two Cu1 atoms, indicating that this sample is a real twin-free crystal.

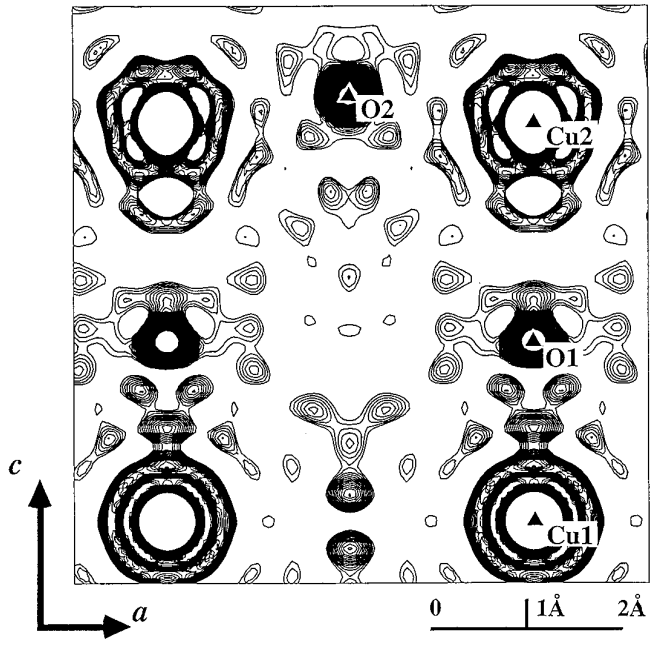

FIG. 4. Fourier map of twin-free YBCO crystal shown in the (010) plane at $y = 0$. Contour intervals 1 eÅ^{-3}. Contours in positive regions are solid and negative regions and zero contour is omitted.

There are two electron density peaks between two Cu1 atoms along the *a* axis which are vacancy sites (Fig. 4). These two electrons were also checked in the refinement procedure by decreasing the occupancy of Cu1, and it was found they belong to the Cu1 atom and not the O1 atoms. These two electrons are shared between two Cu1 atoms along the *a* axis.

In Figs. 3 and 5, the residual peak with $\Delta\rho = 3$ eÅ^{-3} between Cu1 and O1 indicates a chemical bond between these two atoms. Two positive peaks are observed near Cu2 along the *c* axis direction. One is located 0.66 away from Cu2 with $\Delta\rho = 3$ eÅ^{-3}; the other with $\Delta\rho = 2$ eÅ^{-3} is between Cu2 and O1 about 0.62 Å away from Cu2, which results from the electron shift from the negative region with $\Delta\rho = -3$ eÅ^{-3} between Cu2 and O2, about 0.58 Å away from Cu2. This shows that the distribution of the Cu2 $3d_{z^2}$ orbital is not an original dumbbell-like one, but the two electrons in the orbital are localized as a lone pair. Around the O2 atom, there is a positive peak with $\Delta\rho = 3$ eÅ^{-3} along the *c* axis, while there is a wide negative region on the other side of the O2 atoms. This gives a polarization along the *c* axis around O2. On the other hand, there is no polarization around O3 (Fig. 5). Figure 5 shows that the Cu1 atom has the residual electron density with typical distribution of the $3d_{yz}$ orbital, but not of the other *d* orbitals. At the site of O4 a residual positive peak (2 eÅ^{-3}) is observed. In Figs. 3 and 5 there are no obvious bond electrons at the Cu2–O2 and Cu2–O3, but two negative peaks were found between them which was described above.

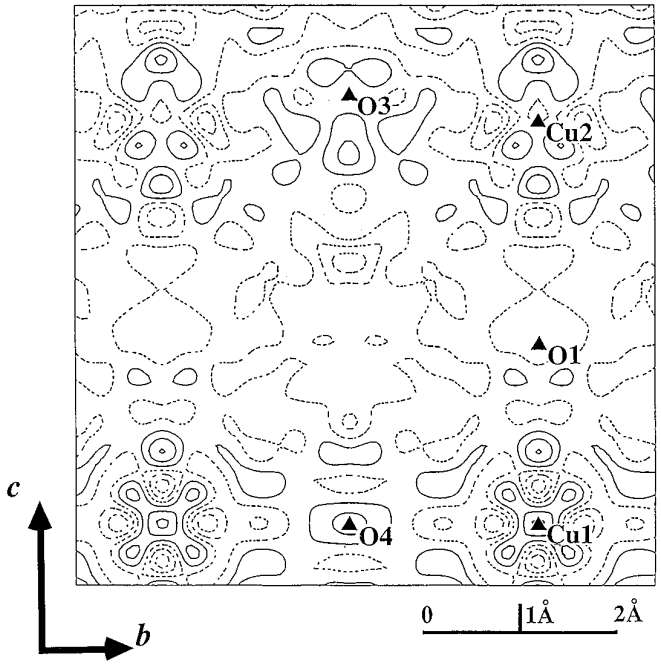

FIG. 5. Fourier difference map of twin-free YBCO crystal shown in the (100) plane at $x = 0$. Contour intervals 1 eÅ^{-3}. Contours in positive regions are solid and negative regions are dashed; zero contour is omitted.

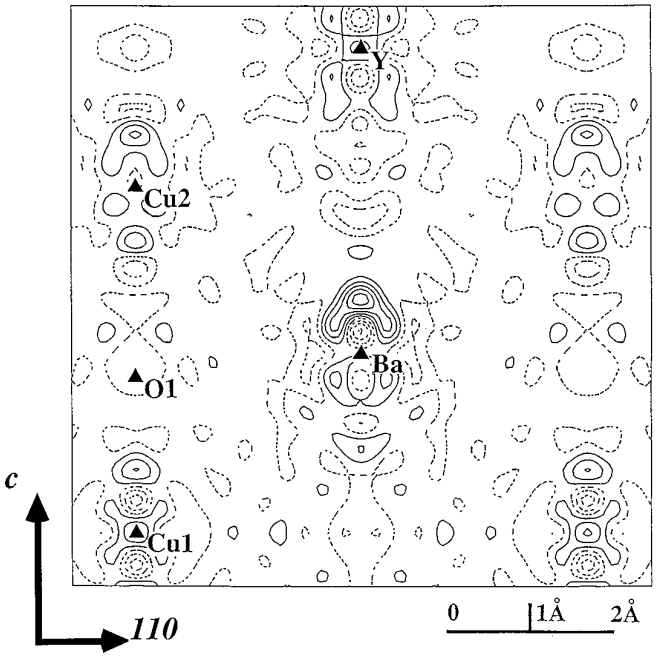

FIG. 6. Fourier difference map of twin-free YBCO crystal shown in the (110) plane. Contour intervals 1 eÅ^{-3}. Contours in positive regions are solid and negative regions are dashed; zero contour is omitted.

No bond electrons were presented between Ba and O1 atoms in Fig. 6, being similar to the case of Cu2–O2. The Ba atom also shows polarization along the *c* axis.

In this work, the electron density distribution is studied only at room-temperature, that is, in the normal state. A comparison of the electron density above T_c with that below T_c would be interesting. This electron density study below T_c is our next target.

CONCLUSION

Twin-free orthorhombic single crystal with $T_c = 91$ K was obtained by applying uniaxial pressure in the oxygen annealing process. Crystal structure of twin-free orthorhombic $YBa_2Cu_3O_{7-x}$ has been determined by a four-circle X-ray diffraction method. The final values of the weighted reliability factor (R_w) and unweighted factor (R) were 0.026 and 0.031. Fourier difference maps were successfully drawn. From these maps, the change distribution and the bonding nature were deduced as follows.

(i) There are differences in the charge distribution between the *a* and the *b* directions.

(ii) The Cu2 atom shows that the distribution of the $3d_{z^2}$ orbital is not an original dumbbell-like one, but localized as a lone pair.

(iii) There are no obvious bond electrons between Cu2 and O2, between Cu2 and O3, and between Ba and O1, suggesting a strong orbital hybridization.

(iv) The O2 atom has polarization along the *c* axis, but the O3 atom does not.

ACKNOWLEDGMENT

This work was supported by the New Energy and Industrial Technology Development Organization for the R&D of Industrial Science and Technology Frontier Program.

REFERENCES

1. M. K. Wu, J. R. Ashburm, C. J. Torng, P. H. Hor, R. L. Meng, L. Gao, Z. J. Huang, Y. Q. Wang, and C. W. Chu, *Phys. Rev. Lett.* **58,** 908 (1987).
2. D. L. Kaiser, F. Holtzberg, M. F. Chisholm, and T. K. Worthington, *J. Cryst. Growth* **85,** 593 (1987).
3. H. J. Scheel and F. Licci, *J. Cryst. Growth* **85,** 607 (1987).
4. K. Dembinski, M. Gervais, P. Odier, and J. P. Coutures, *J. Less-Common Met.* **164–165,** 177 (1990).
5. S. M. Rao, B. H. Loo, N. P. Wang, and R. J. Kelley, *J. Cryst. Growth* **110,** 989 (1991).
6. H. Asaoka, H. Takei, Y. Iye, M. Tamura, M. Kinosita, and H. Takeya, *Jpn. J. Appl. Phys.* **32,** 1091 (1993).
7. Y. Yamada and Y. Shiohara, *Physica C* **217,** 182 (1993).
8. J. S. Kim and D. R. Gaskell, *J. Am. Ceram. Soc.* **77**(3), 753 (1994).
9. G. Roth, B. Renker, G. Heger, M. Hervieu, B. Domenges, and B. Raveau, *Z. Phys. B* **69,** 53 (1987).
10. I. Nakai, S. Sueno, F. P. Okamura, and A. Ono, *Jpn. J. Appl. Phys.* **26,** L788 (1987).
11. R. M. Hazen, L. W. Finger, R. J. Angel, C. T. Prewitt, N. L. Ross, H. K. Mao, C. G. Hadidiacos, P. H. Hor, R. L. Meng, and C. W. Chu, *Phys. Rev. B* **35,** 7238 (1987).
12. S. Sato, I. Nakada, T. Kohara, and Y. Oda, *Acta Crystallogr. C* **44,** 11 (1988).
14. S. Sasaki, Z. Inoue, N. Iyi, and S. Takekawa, *Acta Crystallogr. B* **48,** 393 (1992).
15. S. Sato, I. Nakada, T. Kohara, and Y. Oda, *Jpn. J. Appl. Phys.* **26,** L663 (1987).
16. R. H. Buttner, E. N. Maslen, and N. Spadaccini, *Acta Crystallogr. B* **48,** 21 (1992).
17. A. Simon, K. Trubenbach, and H. Borrmann, *J. Solid State Chem.* **106,** 128 (1993).
18. K. Brodt, H. Fuess, E. F. Paulus, W. Assmus, and J. Kowalewski, *Acta Crystallogr. C* **46,** 354 (1990).
19. P. T. Beurskens, G. Admiraal, G. Beurskens, W. P. Bosman, S. Garcia-Granda, R. O. Gould, J. M. M. Smits, and C. Smykalla, ''The DIRDIF program system.'' Technical Report of the Crystallography Laboratory, University of Nijmegen, The Netherlands.
20. D. T. Cromer and J. T. Waber, ''International Tables for X-ray Crystallography,'' Vol. 4, Table 2.2A. Kynoch Press, Birmingham, England, 1974.
21. J. A. Ibers and W. C. Hamilton, *Acta Crystallogr.* **17,** 781 (1964).
22. D. C. Creagh and W. J. McAuley, ''International Tables for Crystallography'' (A. J. C. Wilson, Ed.), Table 4.2.6.8, p. 219. Kluwer Academic, Boston, 1992.